

**SKB**

---

**TECHNICAL  
REPORT**

---

**87-09**

**Piping and erosion phenomena in  
soft clay gels**

Roland Pusch, Mikael Erlström  
Lennart Börgesson  
Swedish Geological Co, Lund

May 1987

PIPING AND EROSION PHENOMENA IN SOFT CLAY GELS

Roland Pusch, Mikael Erlström, Lennart Börgesson  
Swedish Geological Co, Lund

May 1987

This report concerns a study which was conducted for SKB. The conclusions and viewpoints presented in the report are those of the author(s) and do not necessarily coincide with those of the client.

Information on KBS technical reports from 1977-1978 (TR 121), 1979 (TR 79-28), 1980 (TR 80-26), 1981 (TR 81-17), 1982 (TR 82-28), 1983 (TR 83-77), 1984 (TR 85-01), 1985 (TR 85-20) and 1986 (TR 86-31) is available through SKB.

SWEDISH GEOLOGICAL CO  
Roland Pusch/JS

Date: 1987-05-26  
ID-no: IRAP 87505

PIPING AND EROSION PHENOMENA  
IN SOFT CLAY GELS

Roland Pusch  
Mikael Erlström  
Lennart Börgesson

Swedish Geological Co  
Lund, Sweden

## CONTENTS

	Page
SUMMARY	I
1 SCOPE	1
2 CURRENT CONCEPT	1
3 PHYSICAL MODELS	4
3.1 Piping	4
3.1.1 General	4
3.1.2 Microstructural considerations	7
3.1.3 Theory	7
3.1.4 Comments	10
3.2 Erosion	11
3.2.1 Microstructural considerations	11
3.2.2 Dispersibility	16
4 EXPERIMENTAL	21
4.1 Equipment	21
4.2 Clay material	21
4.3 Test program	23
4.4 Results	23
4.4.1 Test 1, SWY-1, w=1000 %	23
4.4.2 Test 2, SWY-1, w=3000 %	25
4.4.3 Test 3, SWY-1, w=3000 %	27
4.4.4 Test 4, Fyledalen, w=100 %	27
5 DISCUSSION	29
5.1 General	29
5.2 Piping	29
5.3 Erosion	30
5.4 Recommendations	31
6 REFERENCES	32
7 APPENDICES	33

## SUMMARY

The present study has confirmed the conclusions from earlier investigations of piping and erosion of soft smectite gels by showing that the erodibility can be predicted by comparing the drag forces exerted by flowing water and the cohesive particle bonds in the gels.

Optical microscopy used to identify the detailed erosion mechanisms shows that discrete flakes are not eroded as assumed earlier. The minerals torn off from the gels in fact consist of stable aggregates sized 5-50  $\mu\text{m}$  in the case of electrolyte-poor water and even larger units in ocean-type water. The theoretical model as well as the experiments show that erosion is initiated at a flow rate of  $10^{-4}$  m/s in the first-mentioned type of water and that it becomes significant at  $10^{-3}$  m/s. In salt water the gels are much more erosion-resistant.

Piping, which preceded the erosion in the tests, can take place in the form of radial expansion of natural pore passages in the gels, or by tensile failure, depending on the boundary conditions. Theoretically, the critical pressure to produce piping is about 1 kPa at a water content of 1000 % of Na montmorillonite and this appeared to be on the same order of magnitude as the experimentally determined values for the very conservative conditions that were applied. Separate tests of a clay rich in hydrous mica showed much less erodibility and higher piping resistance than of the smectite gels.

## 1 Scope

The sealing efficiency of montmorillonite gels in rock fractures is essentially a matter of their ability to resist "piping" and erosion by flowing groundwater. Earlier investigations have shown reasonable agreement between laboratory erosion experiments and gel strength estimations, the latter being based on viscometer tests and simple microstructural models. The exact mechanisms involved in the tearing-off and transport of clay particles were not revealed by these macroscopic erosion tests, however, and an additional study, reported here, was initiated to get a deeper insight in these phenomena. Primarily it involved development of a suitable light-microscope technique, and a basic investigation of the two processes piping and subsequent channel erosion.

## 2 Current concept

We are concerned here with soft montmorillonite gels such as clay grouts, which have penetrated rock fractures, either by controlled injection or by expansion from large volumes of dense, saturated Na bentonite, like those in KBS 3 canister deposition holes, or plugged boreholes, shafts and tunnels (1).

Piping, which is the term for local, fast penetration of water creating continuous passages through a soil, is usually considered in connection with the determination of erosion resistance and washing out of very fine particles. In soil engineering practice, particular emphasis has been put to the development of techniques for characterizing this soil property and to the identification of the physico/chemical processes that determine the degradation and transport of soil particles once piping has been established. An often used standard technique to determine the erodibility is the "pinhole test", in which the cylindrical soil sample is confined in a little cell and an axial "pinhole" made through it to initiate water flow under a successively increased hydraulic gradient. Fig 1 illustrates a version which was found to be suitable for investigating smectite-rich clays in a pilot study (2).

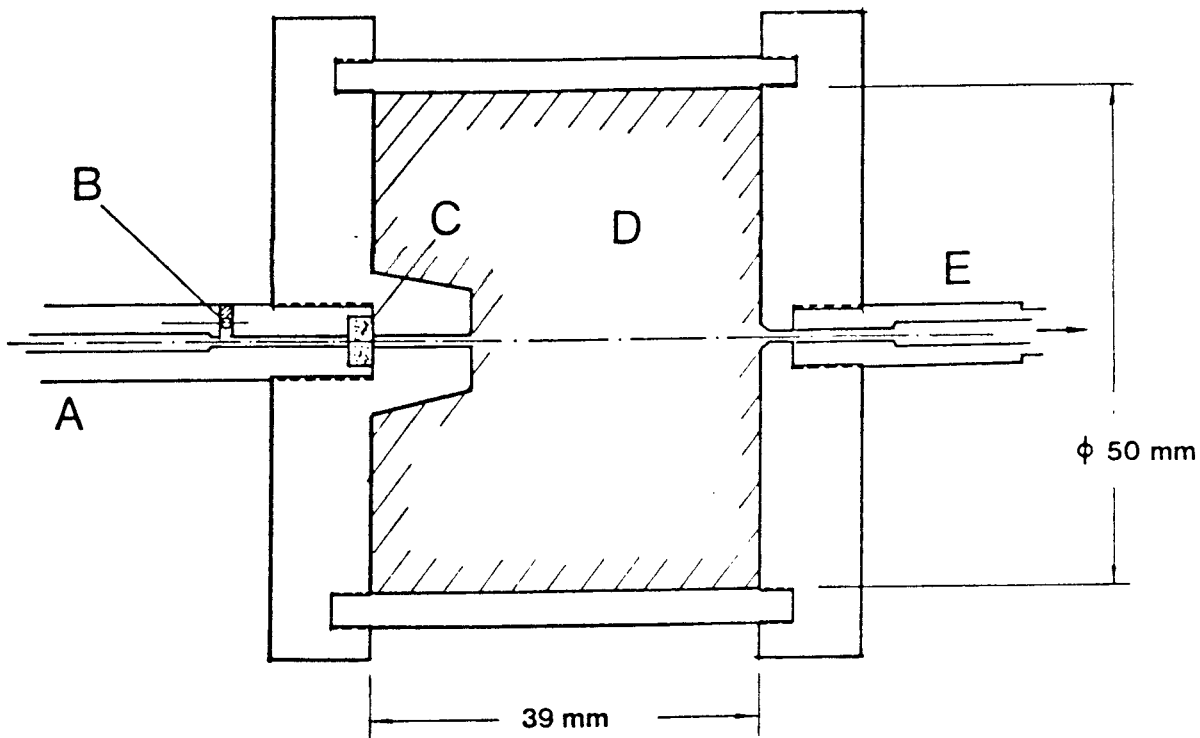


Fig 1. Schematic section through the pinhole test device.  
 A) Inlet nozzle, B) Overflow exit, C) Porous glass filter,  
 D) Clay gel, E) Exit. Before starting the percolation a  
 $\varnothing 1$  mm pin is pushed through the sample along its axis.  
 The nozzles are then applied and the sample left to rest  
 for 30 minutes before the water pressure is raised

Dispersion of expansive clays is known to be largely affected by the so-called sodium adsorption ratio (SAR) of the pore fluid which is defined as  $SAR = Na / \left( \frac{\sqrt{Ca + Mg}}{2} \right)$ , where the chemical symbols refer to the concentrations of the designated cations in milliequivalents per liter. The dispersibility of such clays is also related to the ESP value, which is expressed as  $ESP = (Na/CEC) \times 100$  where Na stands for the sodium concentration in the exchange complex and CEC is the total exchange capacity, both expressed in milliequivalents per 100 g dry clay. Very low SAR and ESP values (<5) are typical of non-dispersive clays, while higher values than 15 characteristically point to strong slaking. Experience from pinhole tests shows that clays tested with sodium ions occupying more than about 10 percent of the exchange complex exhibit dispersion provided that the electrolyte concentration of the fluid has a normality that is lower than  $10^{-3}$ , which is also in agreement with observations from earth dam construction work. This suggests that soft Na smectite gels in rock fractures should be very sensitive to erosion if the water flow rate is significant.

The erodibility can be derived quantitatively by considering the involved physics and such an approach was made a few years ago by calculating the drag forces caused by flowing water and comparing them with the interparticle bonds of a very dilute gel front (2). The average particle bond strength derived from viscometer tests was concluded to be on the order of  $10^{-13}$  -  $10^{-12}$  N for porewaters of low salinity, while the drag force was found to be in the interval  $10^{-15}$  and  $10^{-11}$  N for particles ranging in size from  $0.1 \mu\text{m}$  to  $2.0 \mu\text{m}$  when the flow rates ranged between  $10^{-6}$  and  $10^{-3}$  m/s. The drag forces were calculated by applying Stoke's law assuming the particles to be of spherical shape, i.e. adopting the "Stoke diameter" concept:

$$F = k_1 \cdot \eta \cdot v \quad (1)$$

where  $k_1 = 3 d$  for spherical particles  
 $d$  = Stoke diameter  
 $\eta$  = viscosity of the water  
 $v$  = flow rate

Such theoretical considerations indicated that water flow through or along the front of a clay gel of the type shown in Fig 2 would not tear off particles smaller than  $0.5 \mu\text{m}$  at flow rates lower than about  $10^{-4}$  m/s, and "pinhole" tests appeared to confirm this. The assumption of disc-shaped, discrete particles coupled in an edge-to-face fashion was taken as a first approach in this pilot study, while there are reasons to believe that particles torn off from smectite gels are in fact fairly large, approximately spherical aggregates composed of flaky montmorillonite crystallites.

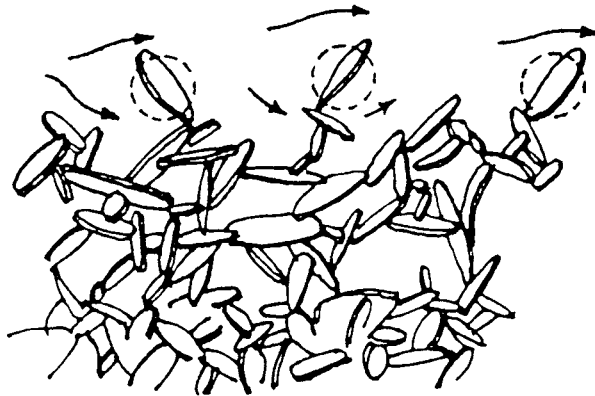


Fig 2. Schematic view of clay gel front exposed to drag forces produced by flowing water



The pinhole tests indicated that piping of soft MX-80 clay in distilled or very weakly brackish water was initiated at a "critical" hydraulic gradient of  $10^{-1}$  when the water content was 435 %, while it was only  $10^{-2}$ - $3 \cdot 10^{-2}$  at a water content of around 1000 %. At a water content of 2000 % (very weakly brackish water) the critical gradient was also found to be about  $10^{-2}$ . The experimental procedure means that the values do not refer to undisturbed clay but to gels which had been punctured and disturbed by the pin and left to homogenize for 30 minutes before percolation started. Due to the involved time-dependent thixotropical regain the physical state of the penetrated central parts of the clay samples was not well defined and a more adequate way of determining the critical gradient was therefore asked for in the present study. This called for the application of a different experimental technique.

### 3 Physical models

#### 3.1 Piping

##### 3.1.1 General

Piping can be produced in different ways depending on the microstructure of the soil. In the case of mixtures of coarser grains and a small amount of clay, the grading of the first-mentioned constituents is a determinant of the water pressure conditions at which piping takes place. Thus, with a Fuller-type grading curve, smaller grains and clay aggregates are effectively supported and prevented from being transported in the pores (Fig 3). If the grading is not proper or the mixture not thoroughly homogenized, or if the amount of clay is not sufficient to fill up the ballast pores with a homogeneous clay gel, soft parts of the gel can be displaced and torn-off fragments transported through channels that are formed at a relatively low water overpressure. Depending on the degree of continuity of the larger voids and the magnitude of this overpressure the displaced gel or individual particle aggregates may clog the channels temporarily and intermittently and thereby cause time-dependent variations in flow rate and hydraulic conductivity.

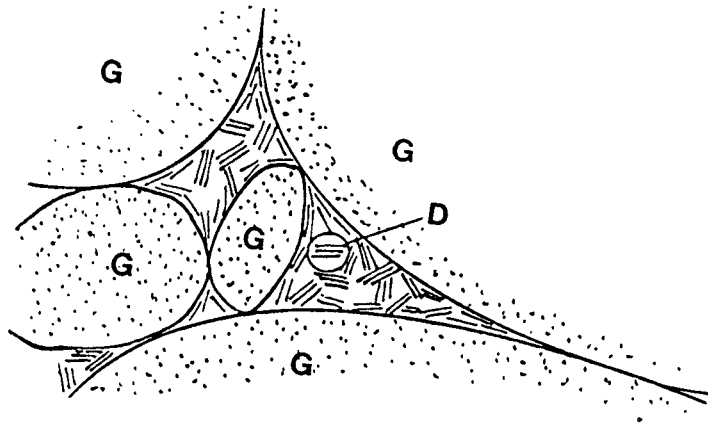


Fig 3. Schematic grain arrangement in the clay/ballast mixtures:  
 G = ballast grains, D = clay aggregate

Clays produced by compacting bentonite powder grains will, in principle, consist of integrated continuous networks of dense and impermeable aggregates, and zones of permeable clay gels, respectively. The density of the latter can be assumed to vary with their size and the piping resistance therefore depends on this variation and on the homogeneity of the gels as in the case of clay-poor mixtures. Thus, at a sufficiently high overpressure, water penetrates soft gels displacing weak zones and transporting clay particle aggregates, thereby causing the same type of gradient- and time-dependent variation in hydraulic conductivity as in clay/ballast mixtures (cf. Fig 4). The effect is naturally most significant in the case of strongly heterogeneous clay gels of very low density.

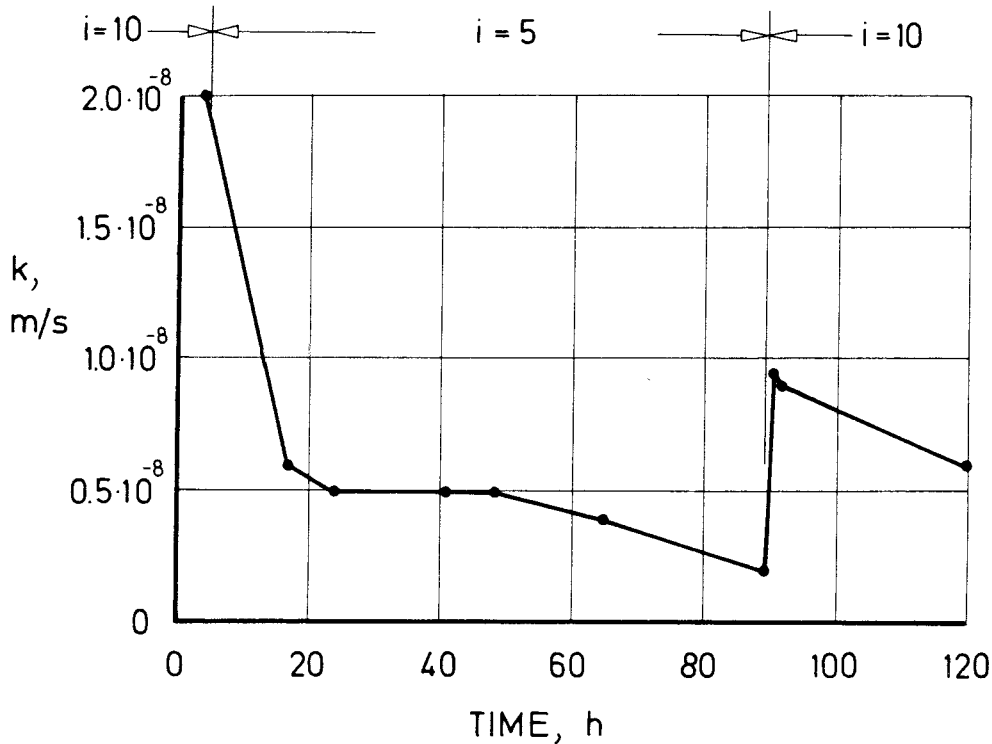


Fig 4. Example of gradient- and time-dependent change in hydraulic gradient of a soft Na-montmorillonite gel (GEKO/OI-bentonite with a bulk density of  $1.3 \text{ g/cm}^3$  in water saturated state: strongly brackish water)

In relatively homogeneous gels, like the ones formed by smectite-rich clay of a density corresponding to that of the Atterberg liquid limit, i.e. about 500 % for a relatively pure Na montmorillonite, piping can be assumed to take place either in the form of radial expansion of existing pore passages, or in the form of "hydraulic fracturing" when the water pressure at the tip of the penetrating water wedge is sufficiently high. In both cases, the "critical pressure" is expected to be related to the existence of microstructural heterogeneities and to the mechanical strength of the clay as shown in the subsequent text.

### 3.1.2 Microstructural considerations

Current investigations of the microstructure of soft clay gels demonstrate that among the many continuous passages that are formed by interaggregate voids, there is always a few wider ones in which water flows at a relatively high rate and which can be enlarged by plastic deformation or splitting by tensile fracturing of the surrounding gel. The average diameter of such passages is strongly dependent on the gel density, the largest ones probably being 0.2-1  $\mu\text{m}$  for gel concentrations ranging between 1.1 and 1.3  $\text{g}/\text{cm}^3$ , i.e. for water contents on the order of 200-600 %. For gels with water contents in the interval 1000-3000 %, with which we are particularly concerned, the largest passages can be assumed to be 5-50  $\mu\text{m}$ . The existence of this kind of passages is considered as a prerequisite for the development of piping in our physical model.

### 3.1.3 Theory

Piping may take place in the form of radial expansion of an initial tube-shaped passage, or as a splitting of such a passage to form a fracture (Fig 5).

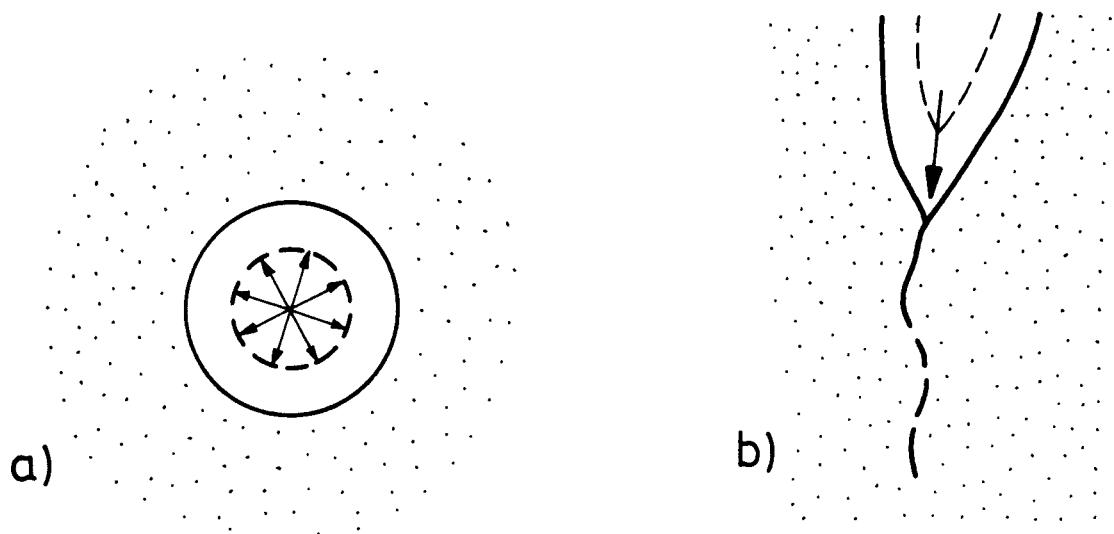


Fig 5. Piping through radial expansion (a) or by "hydraulic fracturing" (b)

"Radial expansion"  
 .....

The first case can be theoretically treated by considering the material to be elastoplastic. Using Fig 6 and the following definitions, the expressions in Eqs. 1-7 are obtained for plane strain conditions (3).

a = initial radius

c = radial extension of plastic zone

p = internal pressure

u = radial displacement

r = radial distance to considered element

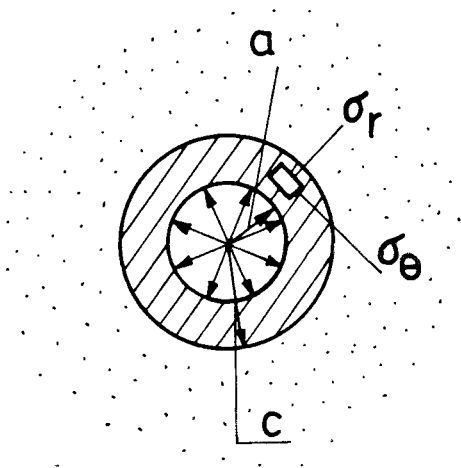


Fig 6. Plastic deformation of zone around cylindrical passage

Plastic condition  
 .....

$$\sigma_r - \sigma_\theta = 2\tau_{fu} \quad (1)$$

where  $\tau_{fu}$  is the undrained shear strength of the gel.

Elastic zone ( $r > c$ )  
 .....

$$\sigma_r = -\tau_{fu} (c/r)^2 \quad (2)$$

$$\sigma_0 = \tau_{fu} (c/r)^2 \quad (3)$$

$$u = \tau_{fu} (1+\nu)c^2/r \cdot E \quad (4)$$

Plastic zone ( $a \leq r \leq c$ )  
 .....

$$\sigma_r = -\tau_{fu} [1+2 \ln (c/r)] \quad (5)$$

$$\sigma_0 = \tau_{fu} [1-2 \ln (c/r)] \quad (6)$$

$$p = \tau_{fu} [1+2 \ln (c/a)] \quad (7)$$

The extension of the plastic zone and the radial strain, i.e. the ratio of the radial expansion of the cylindrical passage and its initial radius, can be obtained from Eqs. 8 and 9, which have been derived i.a. from the previous sets of equations (4). Approximate values of the shear strength and E-modulus are given in Table 1.

Table 1. Undrained shear strength ( $\tau_{fu}$ ) and E-modulus of bentonite

Water content %	Bulk density g/cm <sup>3</sup>	$\tau_{fu}$ kPa	E kPa
50	1.72	100	5000
75	1.56	50	1000
100	1.46	30	600
150	1.34	15	200
200	1.27	10	100
300	1.19	5	50
500	1.12	2	20
1000	1.06	0.5	5
3000	1.02	0.1	1

$$p = \tau_{fu} \left\{ 1 + 2 \ln \left[ \frac{c}{a} + 0.1 \left( \frac{c}{a} \right)^2 \right] \right\} \quad (8)$$

$$\Delta r/r = \tau_{fu} (c/a)^2 \cdot (1+\nu)/E \quad (9)$$

A simple example illustrates how the internal pressure and gel strength are related to yield expansion to a size that can be regarded as a rapidly percolated channel. Estimating this expansion to correspond to an increase in channel radius from  $a=20 \mu\text{m}$  to  $30 \mu\text{m}$ , which means  $\Delta r/r=0.5$ , and applying the value  $0.50 \text{ kPa}$  of the undrained shear strength of Na-montmorillonite at 1000 % water content and furthermore putting  $\nu=0.5$  and  $E \approx 5 \text{ kPa}$ , we obtain  $c \approx 60 \mu\text{m}$  and  $p \approx 2 \text{ kPa}$ . For 3000 % water content we obtain  $c \approx 60 \mu\text{m}$  and  $p \approx 0.4 \text{ kPa}$ . We see from these calculations that this theory yields values that appear to be reasonable. However, in its present form the theory does not allow for larger deformations, such as those which would correspond to the very significant increase in flow-rate that we would actually term "piping".

### "Hydraulic fracturing"

It has been demonstrated in practice (5) that hydraulic fracturing can be produced in natural clay layers by increasing the water pressure in piezometers. Thus, steeply oriented fractures propagate from the piezometers when the water pressure exceeds the lateral in situ soil pressure and the tensile strength of the clay. Taking the tensile strength ( $\sigma_d$ ) of clay gels to be equal to the compressive strength under undrained conditions, i.e.  $\sigma_d = 2\tau_{fu}$ , the critical internal pressure to initiate fracturing should also be  $2\tau_{fu}$  if external soil pressure is disregarded. Using the same example as in the radial expansion case, we thus expect the critical pressure to be about  $1 \text{ kPa}$  for the gel with 1000 % water content. For the softest gel with 3000 % water content the critical pressure would be about  $0.2 \text{ kPa}$ . Obviously, this approach also yields reasonable values.

#### 3.1.4 Comments

We see from the previous text that both the theory of radial expansion of an elastoplastic medium and the simple case of tensile failure yield similar and reasonable values of the critical pressure for

soft pure clay. The first-mentioned theory implies large strain, by which a porewater overpressure is generated. The "disturbed", plastic zone in which this overpressure is generated is apt to consolidate rapidly, yielding a denser zone at the channel wall and the assumed 50 % increase in channel diameter.

The applicability of the two approaches is strongly dependent on the boundary conditions. Thus, if the gel is not laterally confined, splitting will take place of the gel which would, in principle, remain in an elastic state, while radial expansion in connection with the development of a plastic zone will occur if the gel has a limited lateral extension and is rigidly confined between ballast grains or in rock fractures.

## 3.2 Erosion -----

### 3.2.1 Microstructural considerations

#### General .....

Although the basic principle of relating the drag forces exerted by flowing water to the cohesive forces between adjacent crystallites is relevant in order to predict clay erodibility, the earlier concept of platy particles with a diameter of 0.1-2  $\mu\text{m}$  needs to be revised. Thus, recent investigations demonstrate that what we have previously termed "particles" that are torn off by flowing water are in fact aggregates consisting of thin stacks of montmorillonite flakes and these aggregates have a size and shape that are determined by the groundwater chemistry and the mode of gel formation. These factors also determine the nature and strength of the particle bonds that operate in as well as between the aggregates.

For the sake of simplicity we will still use the term particle for individual microstructural constituents in the subsequent text together with the specifications "flake" and "lamella" for individual crystal sheets, "stack" for aligned, regularly ordered sheets, and "aggregate" for coherent groups of non-oriented sheets and stacks.



High voltage "humid cell" microscopy of the hydration process taking place in initially very dense Na montmorillonite aggregates has demonstrated that single montmorillonite flakes do not exist unless strong mechanical agitation is applied (6). In practice there always seems to be groupings of several flakes in the branches that are formed when montmorillonite gels are free to expand, although the number of flakes that stick together in very diluted Na montmorillonite appears to be as small as 5-10. The general process that leads to such groupings is the hydration of initially dense and large stacks of aligned flakes which expand to hold 2-3 interlamellar hydrate layers in a first swelling stage, and which are broken up in thinner fragments due to mechanical stresses that are set up in the expansion process. Further swelling is thereby initiated if sufficient space is provided. The interlamellar attraction, produced by van der Waals forces, electrostatic bonds and hydrogen bonds, appears to be sufficiently strong to resist complete dispersion.

#### Modes of formation

.....

The way in which the gel is formed is of great significance with respect to its stability. Expansion from a dense state, as in the case of penetration of smectite clay into rock fractures from a dense clay block, partly preserves the face-to-face association of the flakes and yields a system of disc-shaped particles with a tendency to separate spontaneously (A in Fig 7). The system may partly be reorganized to form aggregates with various types of association of the stacks, such as edge-to-face coupling (B in Fig 7). The latter type of microstructural arrangement is also assumed to evolve in thixotropically hardened gels after the strong mechanical agitation that is part of the preparation of clay suspensions for rock grouting. Coagulation (flocculation) occurs when the flakes or thin stacks are free to move in the water after stopping the agitation, their movement being due to rotary and translatory Brownian motion at a large interparticle distance, as well as to mutual charge interaction when the particles are closely spaced. Plate I (Appendices) illustrates two major types of aggregates, representing expanded stacks (A) and coagulated groups of flakes and thin stacks (B).

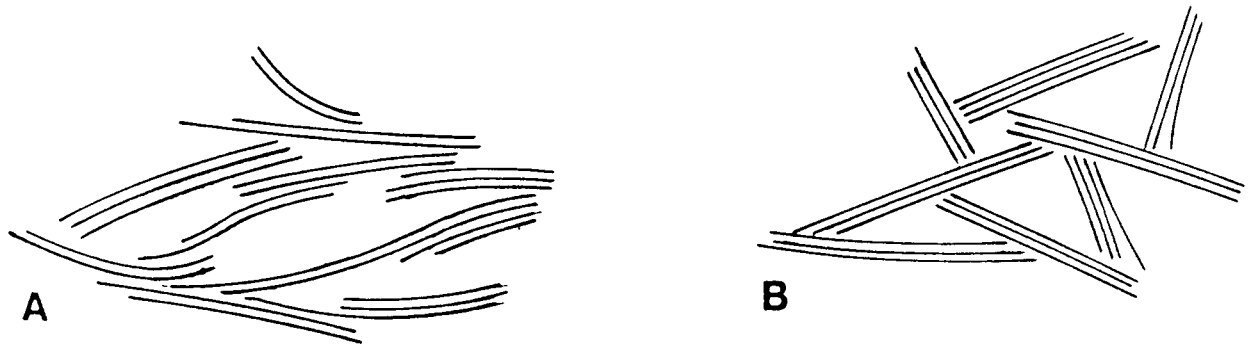


Fig 7. Microstructure of smectite clays at low bulk densities

It can be shown that the course of coagulation is a function of time and a matter of probability (7). Thus, the probability of collision between the particles is of special importance to the coagulation rate and it depends on the collision diameters of the particles. In the case of spherical particles, this diameter is equal to the particle diameter, and in the case of non-spherical particles it is approximately equal to the maximum diameter, which can be more than a thousand times larger than the thickness of a single smectite flake. Since clay particles are markedly flaky the probability of collision is high.

Once the separation distance is sufficiently small, interparticle bonds are created. Their nature has been explained and debated for several decades (cf. 8), possible major attraction forces being 1) electrostatic attraction between positively charged edges of thin stacks and negatively charged basal planes of neighboring stacks, 2) polyvalent adsorbed cations establishing bonds between adjacent nearly edge-to-edge and face-to-face coupled stacks, 3) van der Waals forces, and 4) hydrogen bonds between edge-to-edge and face-to-face associated stacks, respectively. The possible existence of shallow secondary minima in potential energy curves of superimposed van der Waals attraction and double layer repulsion of interacting particles has a special bearing on coagulation initiated by Brownian movement in electrolyte-poor water. Thus, it has been suggested that coagulation at the secondary minimum becomes more important than that at the primary minimum as the concentration of cations in the water decreases and as the particle size increases (8). For large smectite flakes or thin stacks of flakes, coagulation at the primary minimum,

i.e. at a small interparticle distance, would actually require 1 mole per liter of Li- or Na- electrolytes while it would only have to be 1/1000 of that concentration to initiate gel formation at the secondary minimum. This is in perfect agreement with the experience that even suspensions with a gel concentration as low as  $1.01 \text{ g/cm}^3$  ultimately form stable gels in practically electrolyte-free ("distilled") water at rest.

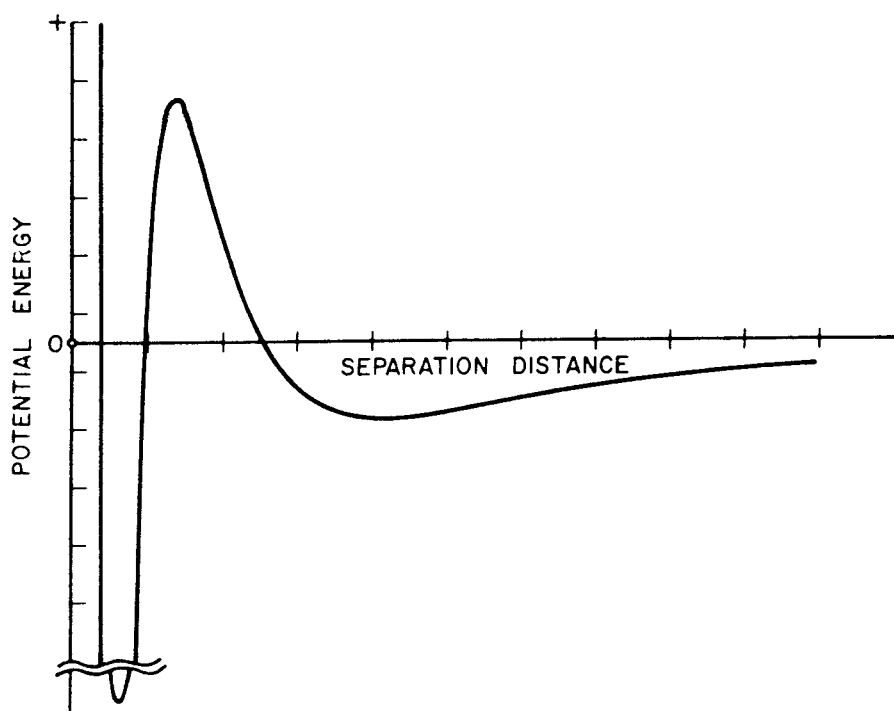


Fig 8. Potential energy versus interparticle distance for two particles in suspension, with two minima in potential energy

The rotary Brownian motion creates a possibility for the thin stacks to approach close enough to make possible an establishment of mutual binding, and it thereby also gives an indication of the type of particle arrangement in the gel formation. Thus, the particle rotation implies that the probability of edge collision is highest for flaky particles which would suggest edge-to-edge coupling between the particles.

Large flakes are always the most anisometric particles, and they are therefore connected at an early stage of the flocculation process, while the smallest, more isometrically shaped flakes or stacks become associated later, through more complex bonding mechanisms. They may predominantly become attracted to the basal planes of the large particles and establish edge-to-face, edge-to-edge and face-to-face coupling with these particles and between themselves. Fig 9 illustrates the size distribution of Wyoming bentonite, which is a natural clay rich in Na-montmorillonite. The size distribution was evaluated from standard sedimentation tests and it does not give a perfectly true picture of the size distribution because of the extreme deviation from spherical shape of the particles.

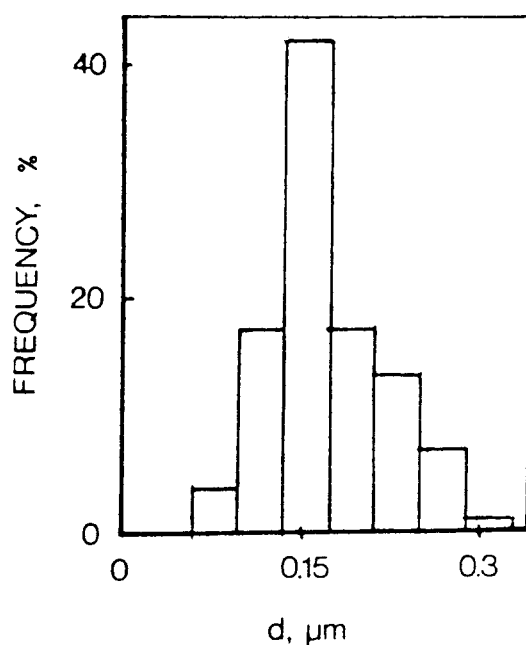


Fig 9. Particle size distribution of Wyoming bentonite. The histogram represents the Stoke diameter of a Na montmorillonite sol that was centrifuged to remove coarser particles. The actual maximum diameter is about 1-2  $\mu\text{m}$  and the ratio between the maximum and minimum diameters is in the range of 10-1000

### Stability of aggregates .....

The smaller particles are more strongly coupled, mutually as well as to the larger particles, and the strongest units of the gel are therefore relatively small flocs or aggregates consisting of a few large particles that are surrounded and connected by smaller crystallites. High electrolyte contents is known to yield stronger aggregates than low ones.

Fig 10, which is valid for illitic clay, illustrates that shear or tension will cause local failure and displace aggregates in a way that yields creep and ultimately bulk shear failure (9). A corresponding image of a smectite aggregate, drawn on the basis of "humid cell" electron micrographs, is given in Fig 11. Assuming that the aggregates do not disintegrate, we can conclude that the smallest clay units that can be removed by flowing water in the course of erosion will have a size which is at least on the same order as the largest individual clay flakes. For natural Na montmorillonites, like smectite-rich commercial bentonite material in distilled water, the minimum diameter of the approximately spherical aggregates is therefore estimated at 2-5  $\mu\text{m}$ , the average size probably being in the range of 10-20  $\mu\text{m}$ . In ocean water the corresponding aggregate size may well be 10 times larger.

### 3.2.2 Dispersibility

As demonstrated in the earlier study, the erosion resistance can be quantitatively estimated by comparing the drag force exerted by flowing water, and the net attraction force that holds individual particles together. Assuming all interparticle bonds to be mobilized simultaneously and to the same extent, one obtains the strength of the individual bonds by dividing the bulk shear strength by the total number of bonds. While the earlier as well as present estimates both point to a probable number of particle bonds of about  $10^{13}$  per  $\text{m}^2$  cross section for a gel density of  $1.06 \text{ g/cm}^3$  ( $w=1000 \%$ ), and  $10^{12} - 5 \cdot 10^{12}$  bonds per  $\text{m}^2$  when the density is about  $1.02 \text{ g/cm}^3$  ( $w=3000 \%$ ), the earlier derived average bond force  $4 \cdot 10^{-13}$  N appears to be too low. Thus, the shear strength figures given in Table 1 yield an average single bond force in the interval of  $10^{-11} - 10^{-10}$  N. Consider-

ing, for the improved model, that the particles consist of stable, spherically shaped aggregates of many tens to hundreds of particles, we arrive at the ratio between drag force and anchoring force that is given by Table 2, taking the bond force as  $10^{-11}$  N. When this ratio exceeds unity, erosion by tearing off aggregates is expected according to this model.

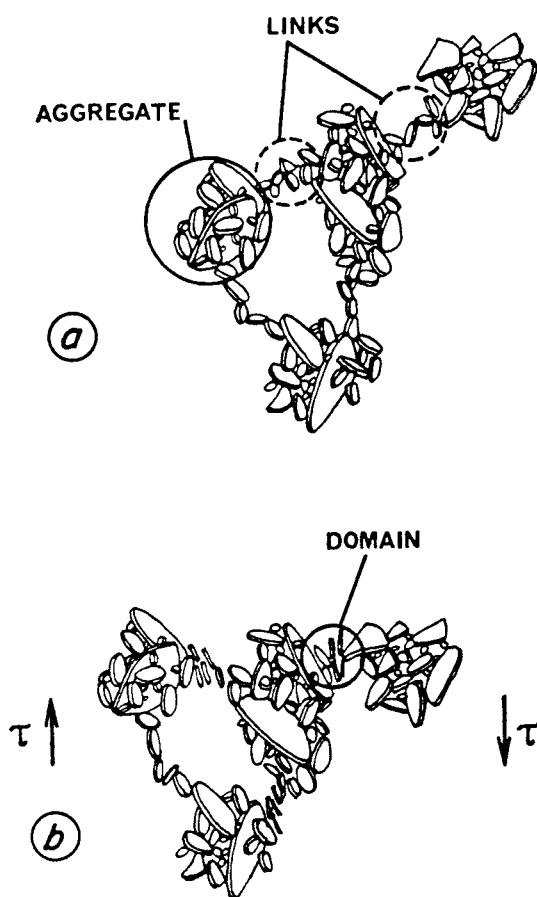


Fig 10. Schematic picture of stable aggregate formed by association of hydrous mica particles in the course of coagulation. a) Natural microstructure of pattern with aggregates forming a coherent gel. b) breakdown of links leading to local failure and release of aggregates

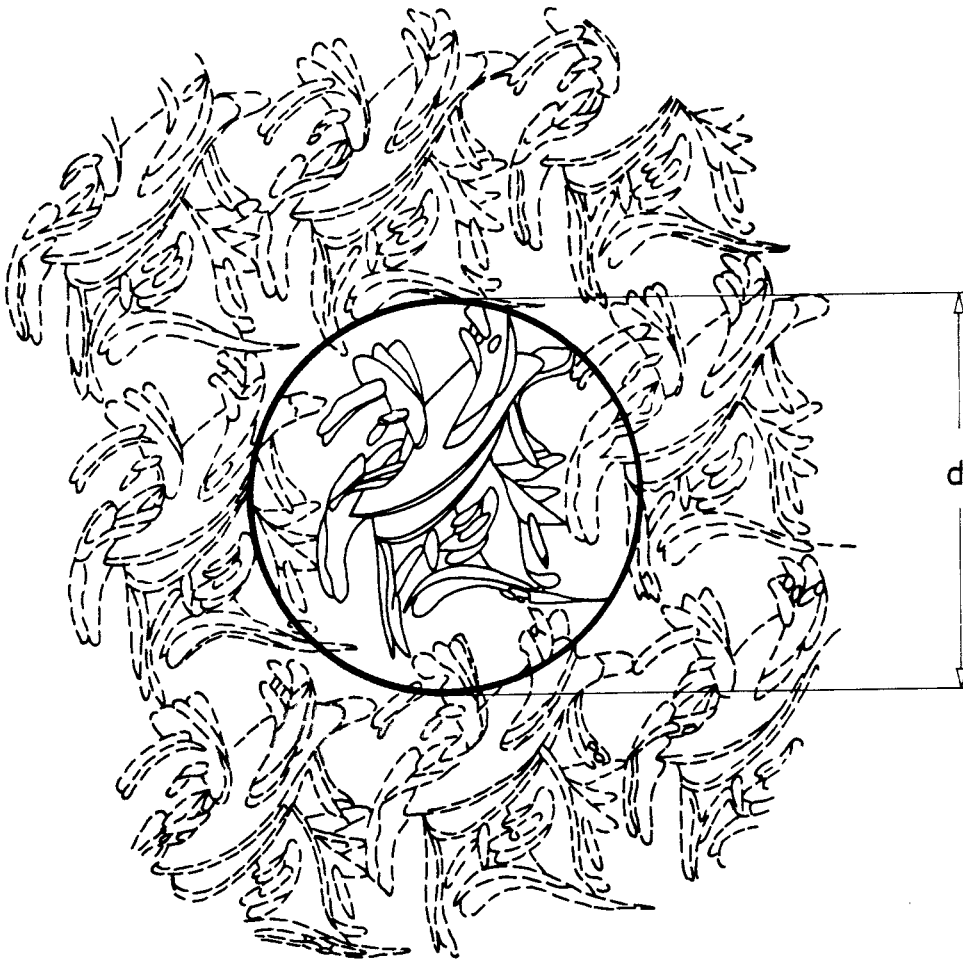


Fig 11. Schematic picture of a smectite "unit" aggregate formed by coagulation,  $d$  typically being in the range of 5-10  $\mu\text{m}$ . The dotted contour depicts an imaginary, coherent clay gel composed of equally sized units in a relatively close packing corresponding to a density of 1.1-1.3  $\text{g}/\text{cm}^3$ . The entire assemblage may be taken as an example of a 20-50  $\mu\text{m}$  roughly spherical aggregate


Table 2 suggests that no erosion is expected for  $n=3$  at flow rates lower than about  $10^{-4}$  m/s. Larger aggregates would tend to be teared off when the flow rate is just about  $10^{-4}$  m/s, while those sized 5-10  $\mu\text{m}$  would not be disrupted unless the flow rate is about  $10^{-3}$  m/s. For highly saline conditions the particle bonds are much stronger than in fresh-water gels and the critical flow rate therefore correspondingly higher.

The ratio  $R$  drops linearly with the number  $n$  of interaggregate bonds and it may be asked what the most plausible figure really is. Electron microscopy studies indicate that the low figure  $n=3$  may be relevant for aggregates with a size of 5-10  $\mu\text{m}$ , as manifested by the schematic drawing in Fig 11, while a higher figure would be plausible for 20-50  $\mu\text{m}$  diameter aggregates. The figure  $n$  should actually be understood as the number of bonds that are activated simultaneously, yielding a "peak" value of the interaggregate strength. Since there is a stochastic variation in actual bond strength and a successive mobilization of the individual bonds at shearing or tension,  $n$  is always considerably smaller than the total number of bonds that can be derived from micrographs.



Table 2. Ratio R of drag force to the anchoring force of aggregates in soft smectite gels under fresh and brackish water conditions and ordinary rock temperature (10-20° C). n denotes the number of interaggregate bonds. Potential risk of flow-induced rupture is marked

Aggregate diameter $\mu\text{m}$	Flow rate m/s	R	
		n=3	n=30
-----			
5	$10^{-6}$	<0.001	<0.0001
10		0.001	0.0001
20		0.002	0.0002
50		0.005	0.005
-----			
5	$10^{-5}$	<0.01	<0.001
10		0.01	0.001
20		0.02	0.002
50		0.05	0.005
-----			
5	$10^{-4}$	0.05	0.005
10		0.1	0.01
20		0.2	0.02
50		0.5	0.05
-----			
5	$10^{-3}$	0.5	0.05
10		1	0.1
20		2	0.2
50		5	0.5
-----			



## 4 Experimental

### 4.1 Equipment

The major aim of the present study was to develop a suitable glass cell for direct observation of the piping and erosion processes of coagulated smectite gels by applying light microscopy. A major requirement was that the glass wall of the slot-shaped cell needed to be 1.5 mm thick at maximum to allow for light microscopy with a reasonably large magnification. Also, the cell had to be sufficiently rigid to resist the maximum internal water pressure, which was estimated at 1-10 kPa. Its nominal aperture was 0.2 mm, the width and length being 20 and 120 mm, respectively.

The cell was connected to burettes for applying a controlled overpressure at one end of the gel, while keeping a low backpressure at the other. A precision flow-meter was integrated to measure and control the flow rate after the development of piping (Fig 12). This device, a Gilmont microflow-meter F3000, operated with an accuracy of  $3 \cdot 10^{-7}$  m/s.

### 4.2 Clay material

Two clay materials were used, one being SWY-1 Na montmorillonite with a smectite content of about 90 % and a maximum size of dispersed clay flakes or thin stacks of 1-2  $\mu\text{m}$ . The other material was a green clay from Fyledalen, Skåne, with hydrous mica as major mineral (60 %) and with rock-forming micas, kaolinite, quartz and feldspars as accessory constituents. This clay was refined by sedimentation to remove particles larger than 2  $\mu\text{m}$ .

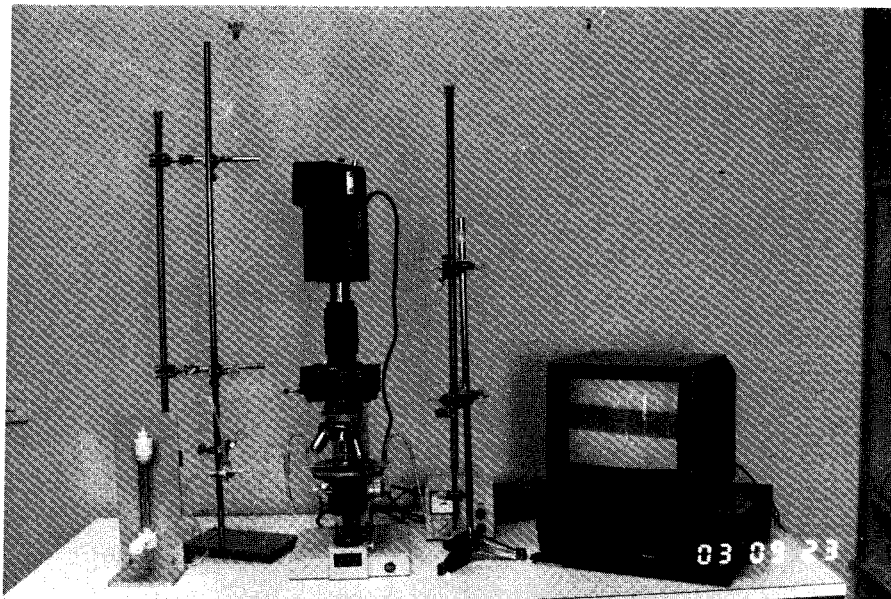
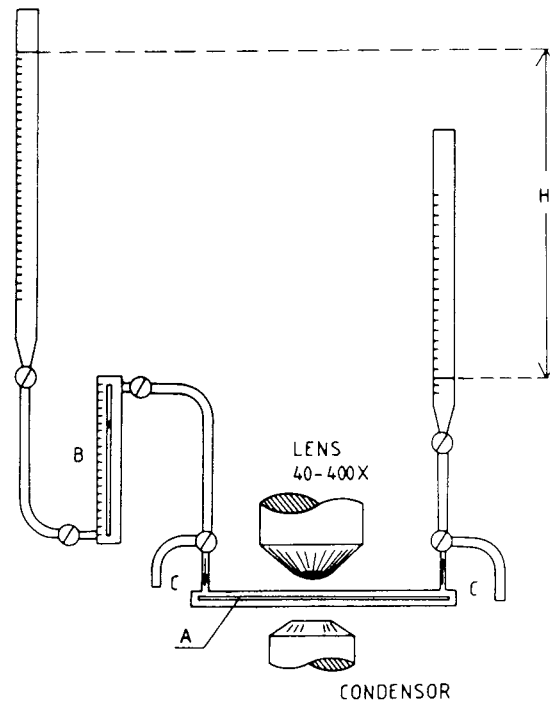


Fig 12. Experimental set-up. Lower picture shows the recording equipment with the video camera attached to the microscope

### 4.3 Test program

The intention was to test homogeneous clay gels with a water content corresponding to the liquid limit. However, they turned out to be too stiff to be introduced in the cell at such a low water content, i.e. 500 % for the smectite and 50-80 % for the Fyledalen clay and higher water contents had to be used, cf. Table 3.

Table 3. Test data

Test no	Clay	Water content %	Density g/cm <sup>3</sup>	Porewater
1	SWY-1	1000	1.06	Distilled water
2	SWY-1	3000	1.02	"
3	SWY-1	3000	1.02	35000 ppm NaCl
4	Fyledalen	100	1.46	Distilled water

### 4.4 Results

#### 4.4.1 Test 1, SWY-1, (w=1000 % distilled water)

The pressure head at the inflow end was successively increased while it was kept low and constant at the outflow end. At a pressure difference of 5 kPa the entire gel mass was slightly displaced and in connection herewith a delta-shaped system of channels was formed (Fig 13). As the most fast-developing branch had penetrated the entire gel mass, forming a main channel, all other branches first became stable and then began to close and become infilled (Fig 14). After the penetration leading to break-through, the flow rate was reduced to practically zero and then successively increased in a controlled way from about  $10^{-6}$  m/s to approximately  $10^{-3}$  m/s.

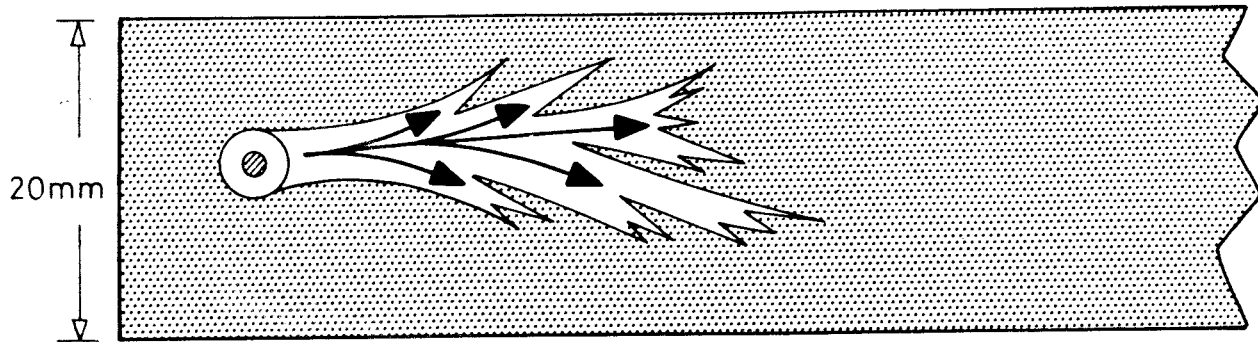


Fig 13. Test 1, SWY-1, ( $w=1000\%$ , distilled water). Initial formation of delta-shaped channel system

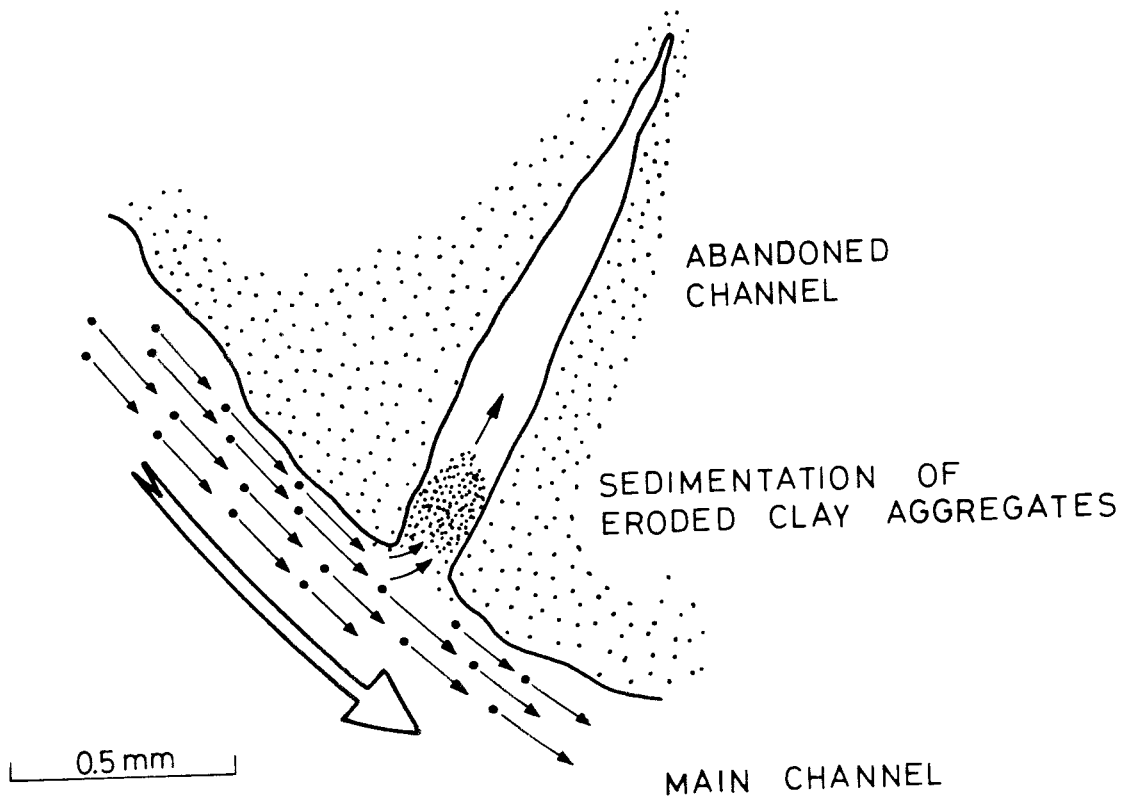


Fig 14. Test 2 SWY-1 ( $w=3000\%$ , distilled water). Infilling of "abandoned" branch after breakthrough of the main channel

Erosion was found to take place at the peripheries of the about 2 mm wide main channel at a flow rate of  $10^{-4}$  m/s. Aggregates sized about 20  $\mu$ m were torn off and moved slowly in a 0.1-0.2 mm shallow zone E along the peripheries (Fig 15). When the flow rate was at maximum ( $10^{-3}$  m/s) the channel was widened to about 15 mm and 20-50  $\mu$ m large aggregates began to be eroded and moved by the water flow. Representative micrographs are shown in Appendix III and IV.

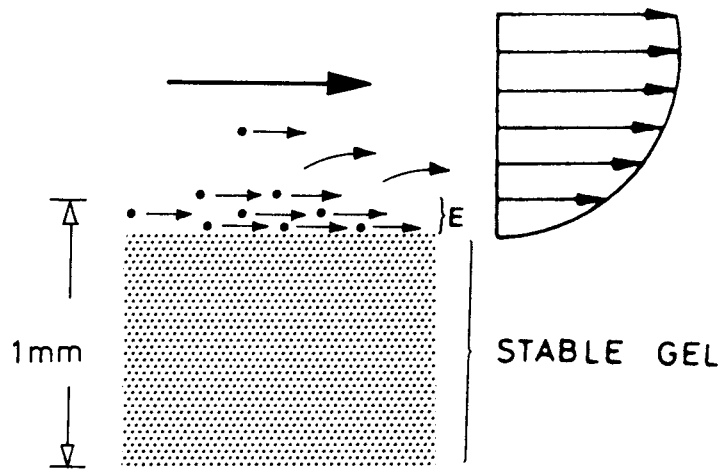


Fig 15. Typical erosion pattern in Test 1

#### 4.4.2 Test 2, SWY-1 (w=3000 % distilled water)

Break-through took place at a pressure difference of about 2 kPa, yielding first a number of branches and finally a main, penetrating channel. After the penetration the same type of healing of the inactive branches took place as in Test 1.

When the flow rate was increased to  $5 \cdot 10^{-4}$  m/s, erosion became obvious in the form of tearing off and migration of 20  $\mu$ m large aggregates in a 0.2-0.5 mm shallow zone along the peripheries of the penetrating channel (Fig 16), and this zone increased considerably when the flow rate was raised to  $6 \cdot 10^{-4}$  m/s. Larger aggregates were then also torn off and the channel finally widened to 15 mm width (Fig 17). Representative micrographs are shown in Appendix V.

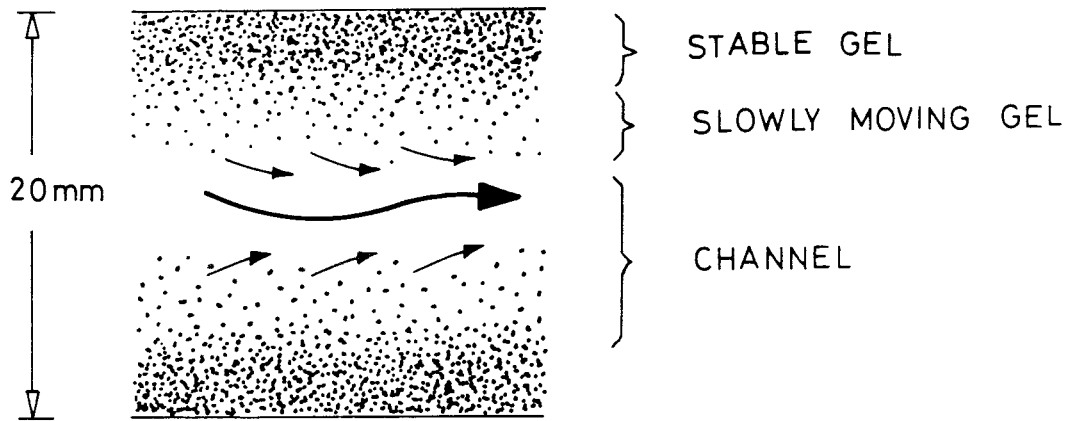


Fig 16. Erosion pattern in Test 2

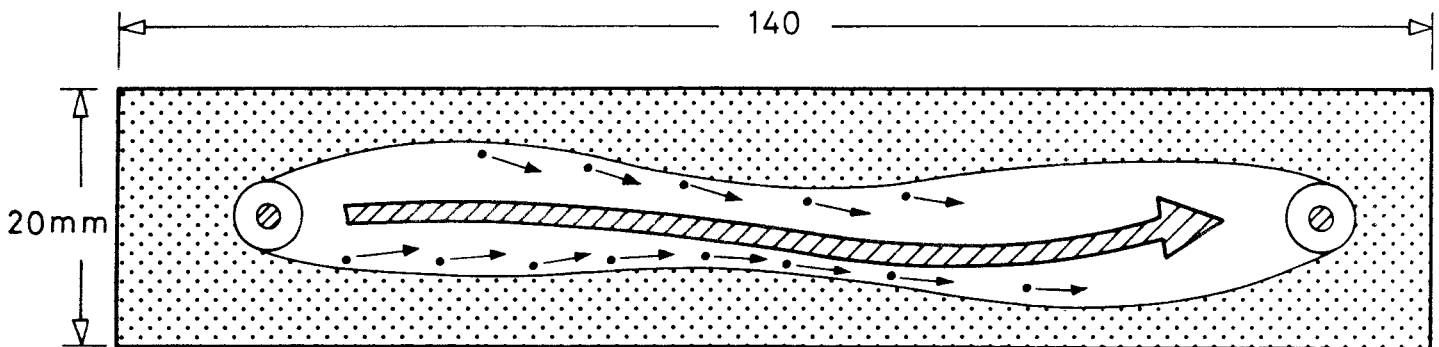


Fig 17. Character of large aggregate transport in Test 2

#### 4.4.3 Test 3, SWY-1 (w=3000 %, 35000 ppm, NaCl solution)

Break-through occurred at approximately the same pressure and penetration rate as for the soft clay dispersed in distilled water, but the general penetration process was more like that of the 1000 % gel in distilled water in the sense that a main, well defined channel was initially developed. There was almost no erosion, however, and not until the flow rate approached  $10^{-3}$  m/s it became significant. It then had the character of separation of very large aggregates, or clay zones, as indicated by Fig 18. Characteristic micrographs are shown in Appendix VI.

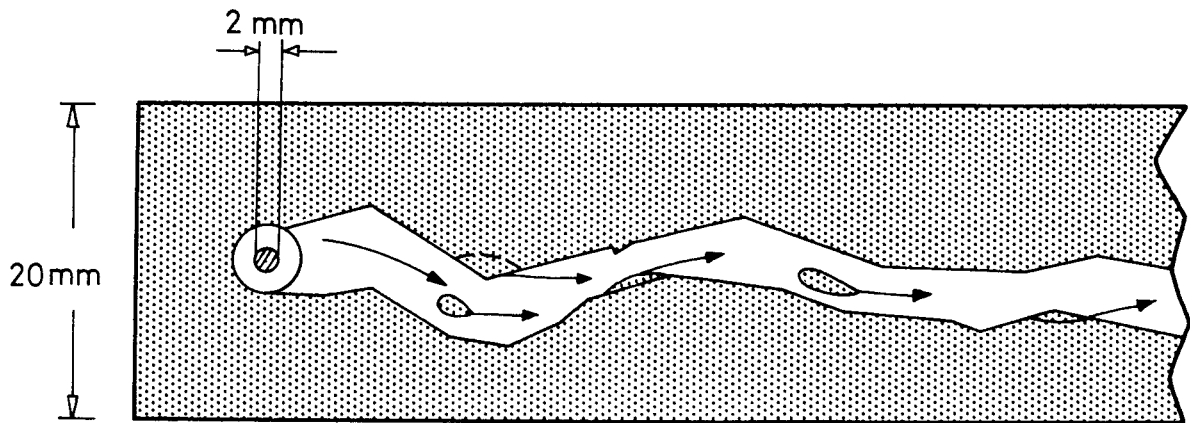


Fig 18. Erosion and transport of large clay zones at the highest flow rate in Test 3

#### 4.4.4 Test 4, Fyledalen (w=100 %, distilled water)

Not even embryotic channel formation took place at the highest pressure head that could be used, i.e. 10 kPa, and suction had to be applied at the outflow end of the cell to produce a penetrating channel, which became about 5 mm wide.

At a water flow rate of about  $10^{-4}$  m/s the channel was successively filled with material eroded from its boundaries, by which the movement of particles tended to stagnate. When the flow rate was increased to  $2 \cdot 10^{-4}$  m/s, the infilling of the original channel started to flow steadily in a zone which was not well defined laterally. At a



flow rate of  $4 \cdot 10^{-4}$  m/s, larger particles and aggregates, sized 10-20  $\mu\text{m}$ , began to move with the finer matrix, and this process became more evident when the flow rate was increased to  $8 \cdot 10^{-4}$  m/s. At about  $10^{-3}$  m/s, a central narrow passage was created, in which relatively pure water flowed (Fig 19). This may indicate that the clay adjacent to the passage successively formed a stable filter by having some clay and fine silt washed out. Characteristic micrographs are shown in Appendix VII.

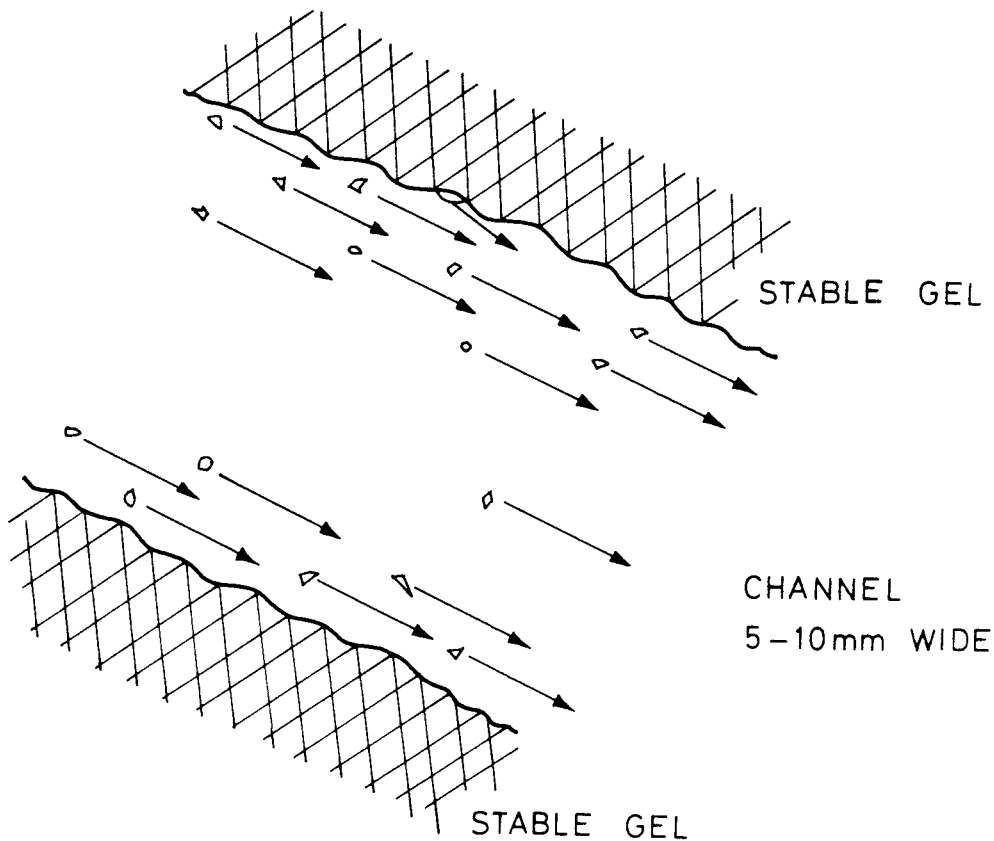


Fig 19. Formation of passage carrying water with few mineral particles at a high flow rate in Test 4. The scale of this picture is much larger than of the previously shown ones

## 5 Discussion

### 5.1 General

The experiments gave a clear picture of the erosion process in soft gels of Na montmorillonite and hydrous mica/kaolinite. The equipment turned out to be useful although it was concluded that the test conditions could only yield piping through tensile failure of the gels and not through radial expansion in combination with plastic strain of the gels.

The predicted microstructural conditions for piping and erosion were validated. Thus, it was found that the majority of the particles that were released from the gels consisted of a large number of particles forming more or less spherical aggregates with a diameter of 5-20  $\mu\text{m}$  in distilled water and more than 10 times that size in salt water. A number of major points are specified in the subsequent text.

### 5.2 Piping

Piping took place in the form of splitting, i.e. through tensile failure, in all the tests and this may well be a general, true phenomenon. It turned out, however, that the deformability of the cell inevitably led to this sort of piping. Thus, at the applied water pressures the cell expanded sufficiently much to allow for the formation of channels without the elastic compression, plastic strain, or consolidation of the gel that are required for the radial expansion case. The conclusion is that the stiffness of the cell needs to be considerably increased in order to offer conditions that are required for the development of piping of this last-mentioned sort.

The recorded water pressure that produced piping through tensile failure in the smectite gels was higher than the predicted critical pressure and it is assumed that this "excess" pressure caused the expansion of the cell that allowed for the development of the observed type of piping. The critical pressure of the smectite gels may therefore have been underestimated. The fact that this pressure was

significantly higher for Fyledalen clay would suggest that its tensile strength is higher than that of the smectite at the respective water content.

We conclude from the study that the piping resistance can be significantly higher if the density is raised. Thus, if rock fractures can be grouted with smectite clay with a water content of 200 %, corresponding to a density of  $1.27 \text{ g/cm}^3$ , the critical pressure can be expected to be in the order of 20 kPa in the case of tensile failure at no lateral confinement. Even higher pressures will be obtained for such relatively stiff gels if they are confined in narrow fractures.

### 5.3 Erosion

The tests confirmed, in principle, that teared-off aggregates have a size of 5-50  $\mu\text{m}$  in electrolyte-poor water and that they are much larger in salt water. Also, fair agreement was found between the actually observed flow rate that produced such gel disintegration and the theoretically predicted critical water flow rate that is required to tear off and transport aggregates of this size. Thus, erosion and transport was found to be initiated at a flow rate of about  $10^{-4} \text{ m/s}$  and when it was increased to about  $10^{-3} \text{ m/s}$  microstructural breakdown became significant and large aggregates torn off. The fact that relatively small aggregates were torn off at the initiation of the erosion while the model predicts that large aggregates would be less stable, can be explained in two ways. The most probable reason is the nature of exposure of the gels to flowing water. Thus, when piping had been produced, water flowed along the plane gel surfaces that were formed and only smaller aggregates could actually be exposed to drag forces over the greater part of their perimeter. Large aggregates had only a smaller part of their outer surface exposed to the flowing water and could therefore not be torn off until surrounding, smaller aggregates had been removed. A second possible explanation, which may actually be related to the first one, is that the number of interaggregate bonds is considerably higher for larger aggregates than for the smaller ones (i.e.  $n \gg 3$ ).

The erosion process and the erodibility appeared to be similar for the smectite gels with 1000 and 3000 % water content when using distilled water, which indicates that the general microstructural pattern is similar for this density range.

All observations fit the general idea of a relatively high but not extreme erodibility of Na smectite clay at low porewater salinity. In brackish or salt water the erodibility is rather low and if smectite is not a major constituent, the resistance to erosion will be strongly increased, as demonstrated by the test of Fyledalen material. An important conclusion was that complete dispersion of soft Na smectite gels does not take place even in very electrolyte-poor water at rest. This means that spontaneous disintegration and loss of smectite clay from grouted fractures will not take place. A water flow rate in the interval of  $10^{-4}$ - $10^{-3}$  m/s will actually be required to cause substantial loss according to the present study.

#### 5.4 Recommendations

Although the present study has demonstrated that the proposed model for erosion is in reasonable agreement with the experimental results, it is not altogether satisfactory. A major weakness is the incomplete understanding of the nature and actual strength of the particle bonds with special respect to the mode of association of neighboring particles. These matters need to be further investigated in connection with the ongoing development of a general rheological model for smectite clays.

As to the critical pressure for initiation of piping, and the basic processes that lead to this form of destruction of clay gels, additional experimental work is required before the validity of the physical model can be judged.

6 References

- 1 Pusch, R., Börgesson, L. & Ramqvist, G. Final Report of the Borehole, Shaft, and Tunnel Sealing Test - Volume III: Tunnel plugging. Stripa Project, 1987 (In press)
- 2 Pusch, R. Stability of Bentonite Gels in Crystalline Rock - Physical Aspects, SKBF/KBS Technical Report 83-04, 1983
- 3 Hill, R. The Mathematical Theory of Plasticity. Oxford University Press, Amen House, London, E. C.4
- 4 Bjerrum, L. & Andersen, K.H. In-situ Measurement of Lateral Pressures in Clay. Proc. 5th European Conf. on Soil Mechanics and Foundation Engineering, Madrid, Vol. 1, 1972 (pp. 11-20)
- 5 Börgesson, L. & Knutsson, S. Programsystem för Lösning av Geoteknisk Spännings- och Flytproblem med Finita elementmetoden. Examensarbete i geoteknik, Lunds Tekniska Högskola, 1972
- 6 Pusch, R. & Karnland, O. Aspects of the Physical State of Smectite-adsorbed Water. SKB Technical Report 86-25, 1986
- 7 Overbeek, J. Phenomenology of Lyophobic Systems. Colloid Science (Part 1), Elsevier Publ Co, 1952
- 8 Bennet, R.H. & Hulbert, M.H. Clay Microstructure, Int. Human Res. Developm. Corp. Boston/Houston/London, 1986
- 9 Pusch, R. Clay Microstructure. Doc. D:8, Nat. Swedish Building Research Council, 1970

A P P E N D I C E S

Micrographs



Plate I. Characteristic smectite particle aggregates in distilled water. The micrographs, which were taken by use of "humid cell" microscopy show fully hydrated particle assemblages (6). The upper picture shows an aggregate consisting of a strongly expanded stack (type A), while the lower one illustrates a coagulated aggregate (type B)

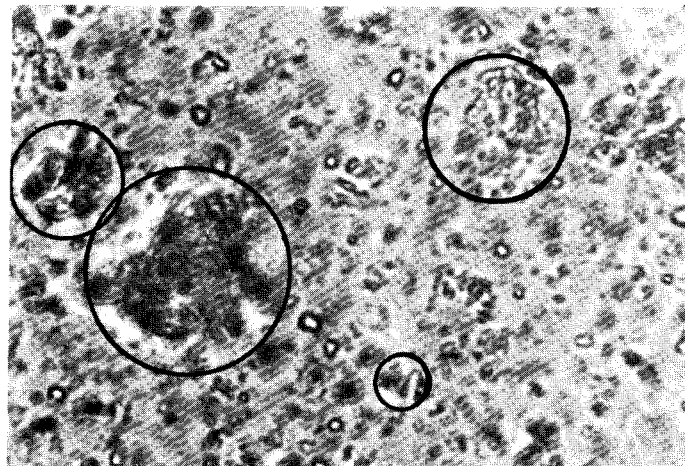
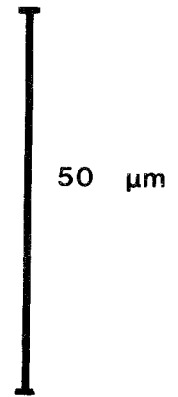
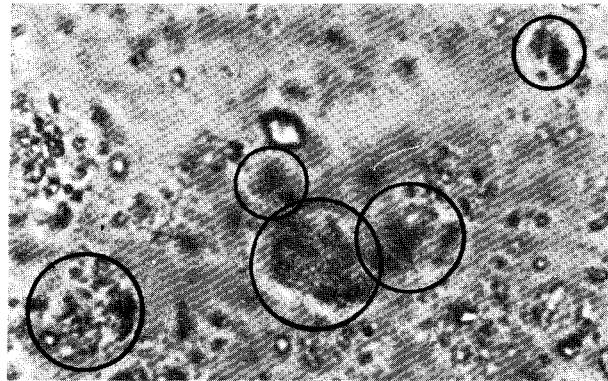


Plate II. Characteristic smectite particle aggregates in distilled water as observed by optical microscopy



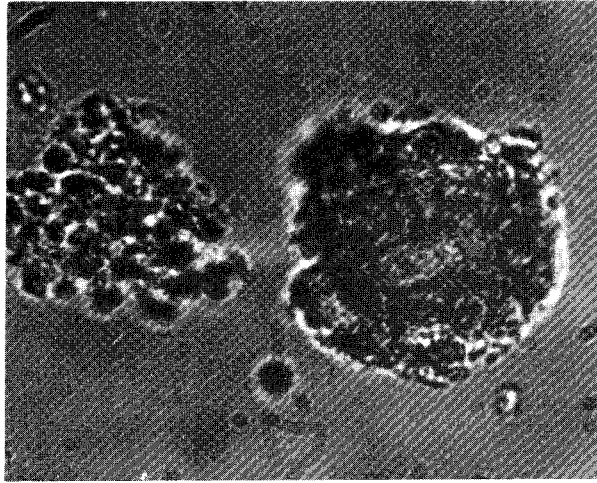
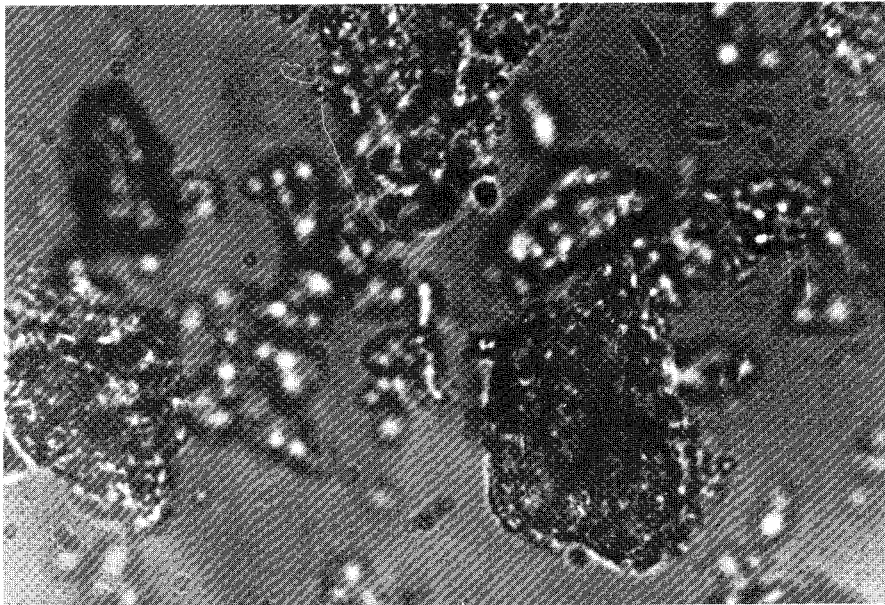
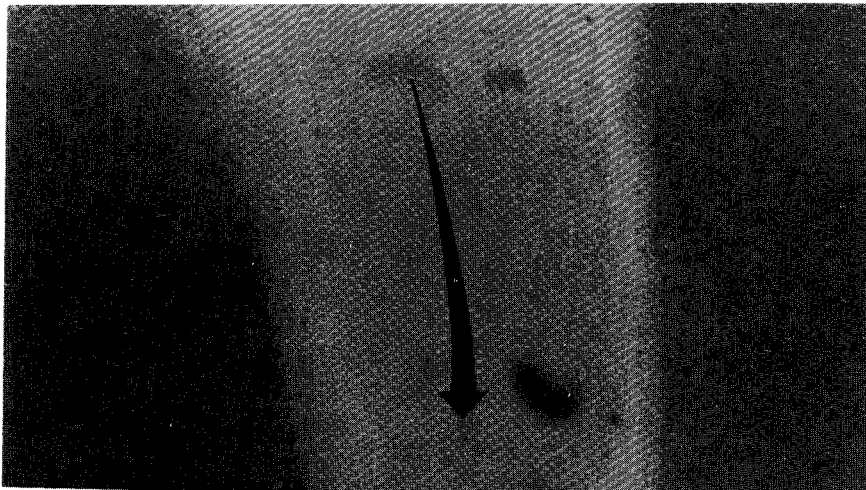
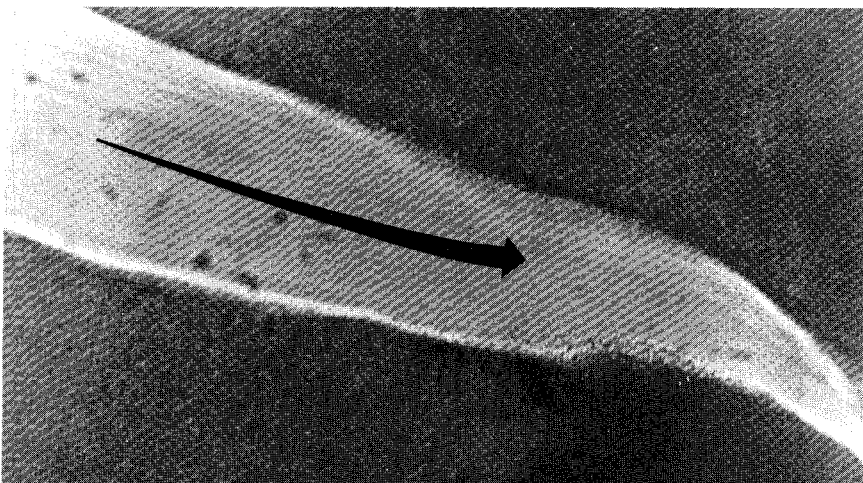
50  $\mu\text{m}$ 

Plate III. Characteristic smectite particle aggregates in 35000 ppm NaCl solution as observed by optical microscopy

## Appendix IV

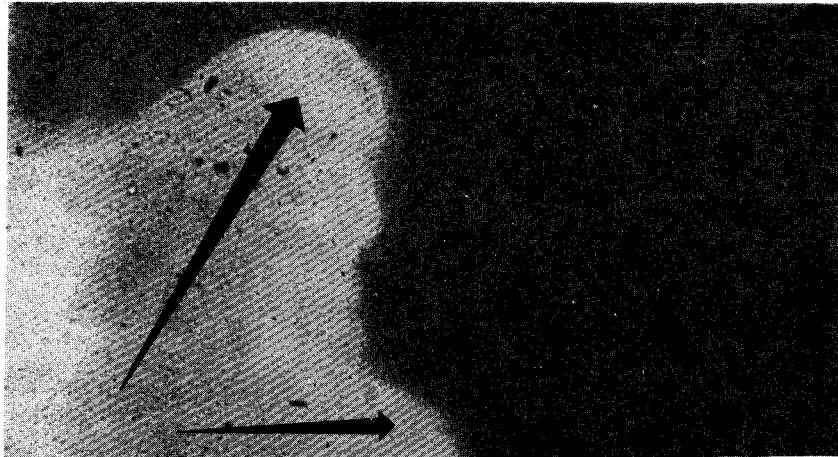
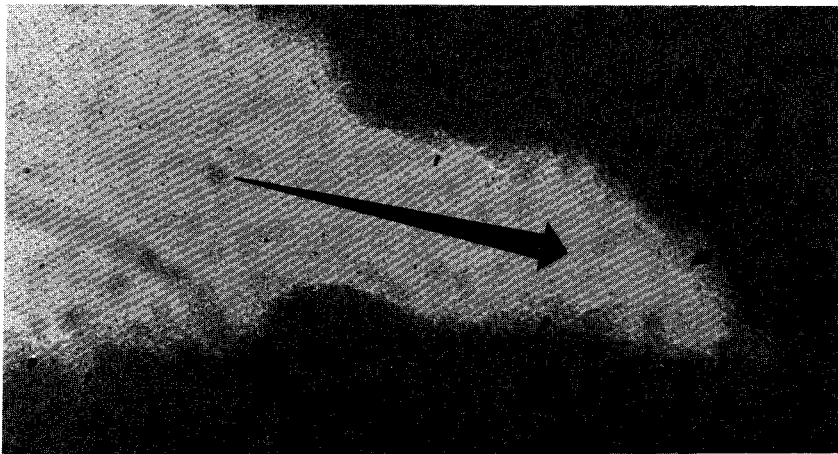
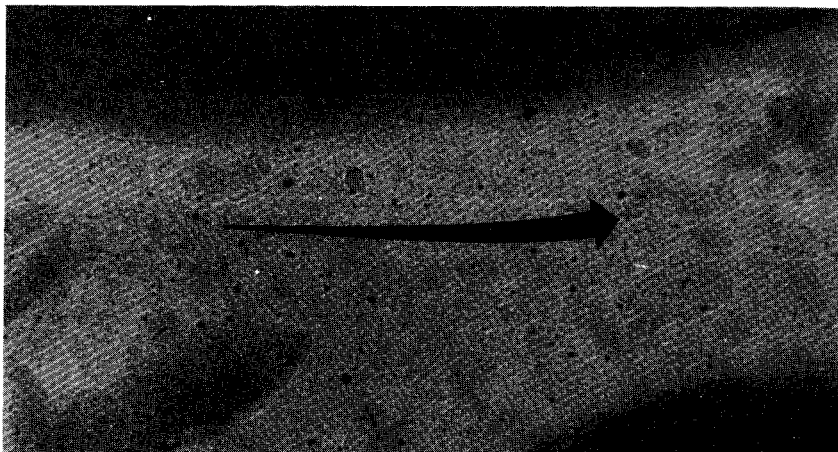
**a****b**

100 μm

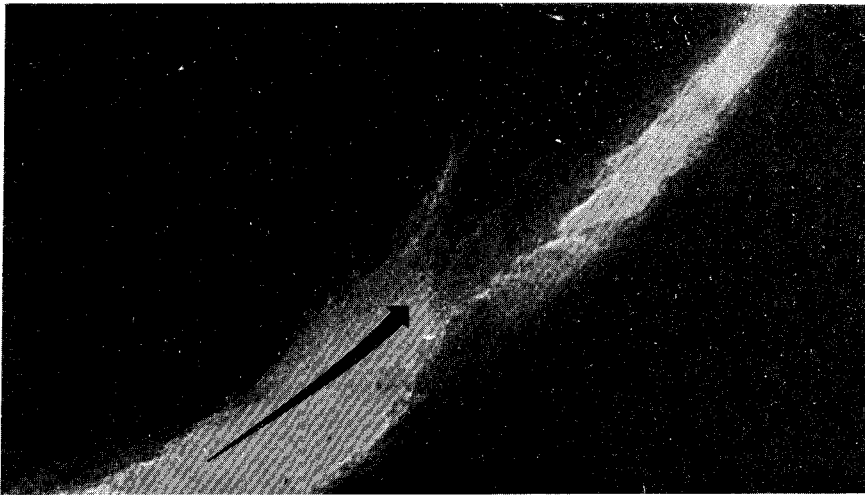
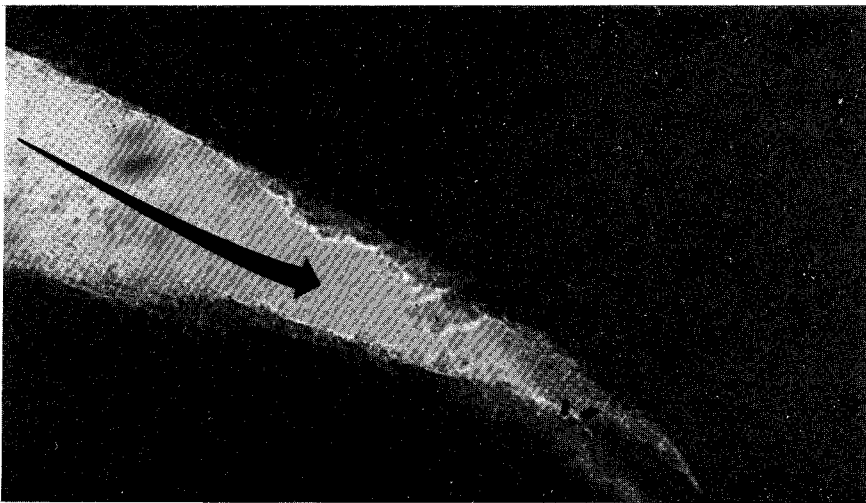
**c**

## Plate IV. Test 1:

- a) Formation of 50 μm main channel in the homogeneous clay gel
- b) Erosion of the clay gel and transport of 10-20 μm aggregates in a boundary zone (E) at a water flow rate of  $10^{-4}$  m/s
- c) 10-50 μm aggregates are torn off and transported at a water flow rate of  $10^{-3}$  m/s

**a**100  $\mu\text{m}$ **b****c****Plate V. Test 2:**

- a) Diffuse irregular shaped channel-front system penetrating the gel
- b) Development of a main channel
- c) Erosion in the main channel at a water flow rate of  $10^{-4}$  m/s

**a****b**

100  $\mu\text{m}$

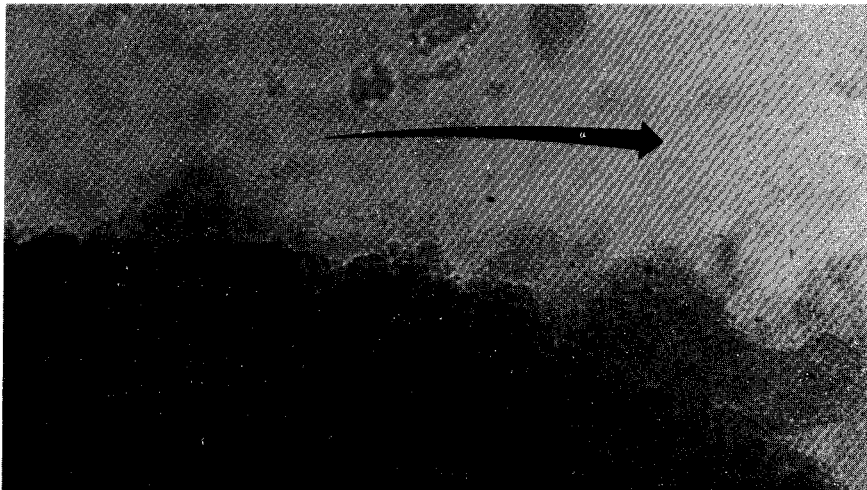
**c**

Plate VI. Test 3:

- a) Formation of 20-200  $\mu\text{m}$  wide channels which penetrate the gel in a branch-like manner until a main channel is developed
- b) Interaction with the protruding saline water causes coagulation of the clay particles at the interface
- c) Coagulation causes significant aggregation of the gel yielding cohesive aggregates of  $>50\mu\text{m}$  size

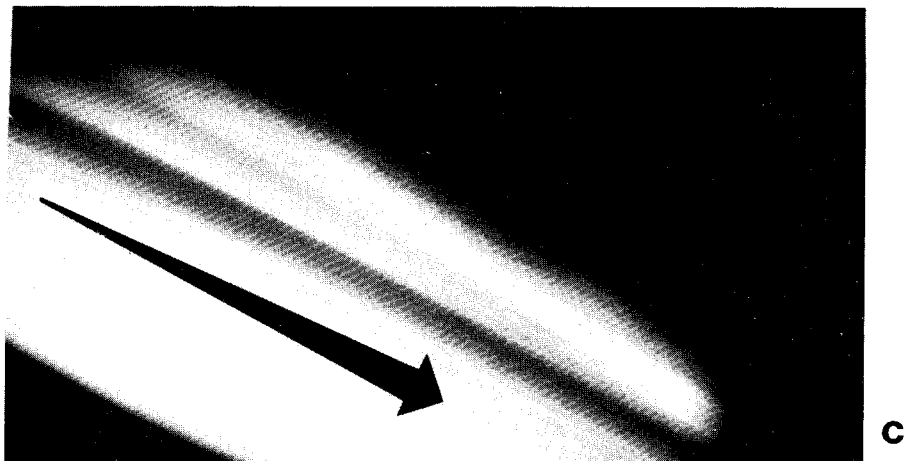
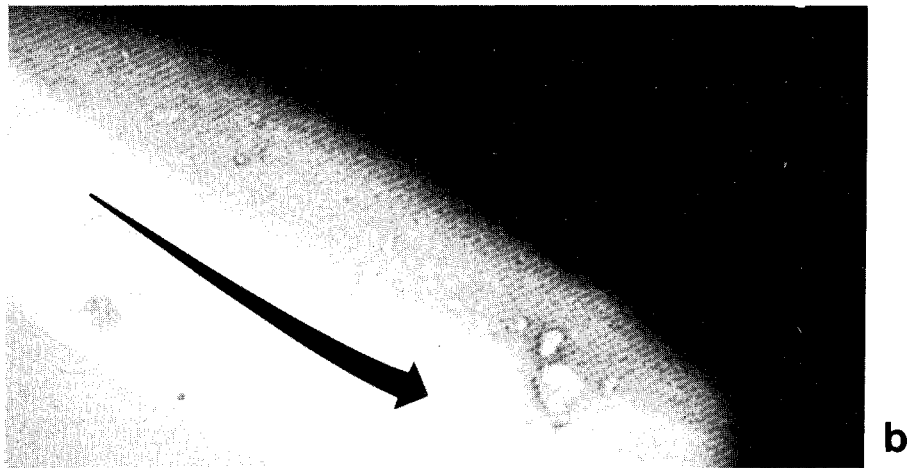
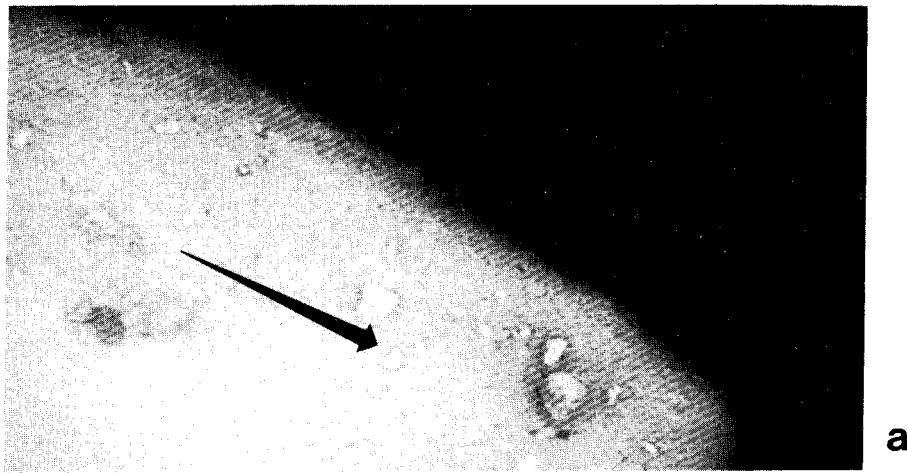


Plate VII. Test 4:

- a) The developed main channel contains initially a relatively homogeneous thin suspension of clay particles and aggregates of 10 μm together with scattered silt sized particles of quarts and mica
- b) Increased flow,  $10^{-4}$  m/s, opens the channel and the central part gets relatively free from particles
- c) At flow rates of  $10^{-3}$  m/s erosion is limited and particle transport concentrated to a few pathways' in the channel

# List of SKB reports

## Annual Reports

1977-78

TR 121

### **KBS Technical Reports 1 – 120.**

Summaries. Stockholm, May 1979.

1979

TR 79-28

### **The KBS Annual Report 1979.**

KBS Technical Reports 79-01 – 79-27.  
Summaries. Stockholm, March 1980.

1980

TR 80-26

### **The KBS Annual Report 1980.**

KBS Technical Reports 80-01 – 80-25.  
Summaries. Stockholm, March 1981.

1981

TR 81-17

### **The KBS Annual Report 1981.**

KBS Technical Reports 81-01 – 81-16.  
Summaries. Stockholm, April 1982.

1982

TR 82-28

### **The KBS Annual Report 1982.**

KBS Technical Reports 82-01 – 82-27.  
Summaries. Stockholm, July 1983.

1983

TR 83-77

### **The KBS Annual Report 1983.**

KBS Technical Reports 83-01 – 83-76  
Summaries. Stockholm, June 1984.

1984

TR 85-01

### **Annual Research and Development Report 1984**

Including Summaries of Technical Reports Issued during 1984. (Technical Reports 84-01-84-19)  
Stockholm June 1985.

1985

TR 85-20

### **Annual Research and Development Report 1985**

Including Summaries of Technical Reports Issued during 1985. (Technical Reports 85-01-85-19)  
Stockholm May 1986.

1986

TR86-31

### **SKB Annual Report 1986**

Including Summaries of Technical Reports Issued during 1986  
Stockholm, May 1987

## Technical Reports

1987

TR 87-01

### **Radar measurements performed at the Klipperås study site**

Seje Carlsten, Olle Olsson, Stefan Sehlstedt,  
Leif Stenberg  
Swedish Geological Co, Uppsala/Luleå  
February 1987

TR 87-02

### **Fuel rod D07/B15 from Ringhals 2 PWR: Source material for corrosion/leach tests in groundwater**

### **Fuel rod/pellet characterization program part one**

Roy Forsyth  
Studsvik Energiteknik AB, Nyköping  
March 1987

TR 87-03

### **Calculations on HYDROCOIN level 1 using the GWHRT flow model**

**Case 1 Transient flow of water from a borehole penetrating a confined aquifer**

**Case 3 Saturated-unsaturated flow through a layered sequence of sedimentary rocks**

**Case 4 Transient thermal convection in a saturated medium**

Roger Thunvik, Royal Institute of Technology, Stockholm  
March 1987

TR 87-04

### **Calculations on HYDROCOIN level 2, case 1 using the GWHRT flow model**

**Thermal convection and conduction around a field heat transfer experiment**

Roger Thunvik

Royal Institute of Technology, Stockholm  
March 1987

TR 87-05

### **Applications of stochastic models to solute transport in fractured rocks**

Lynn W Gelhar

Massachusetts Institute of Technology  
January 1987

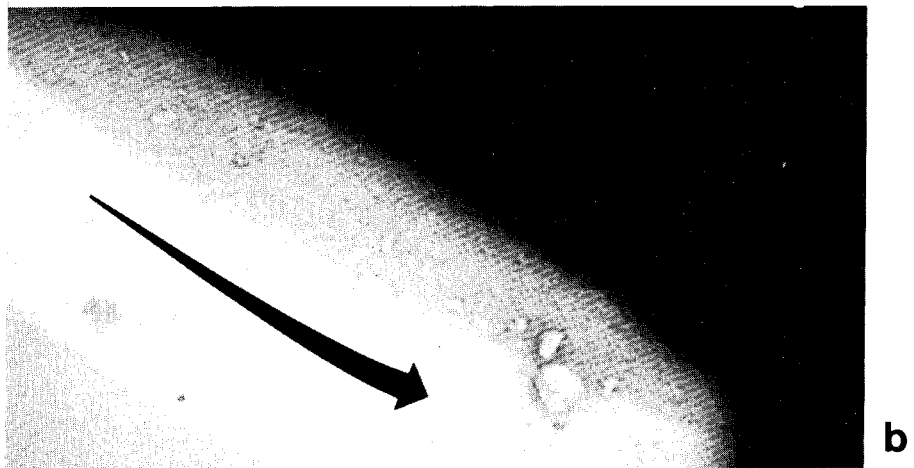
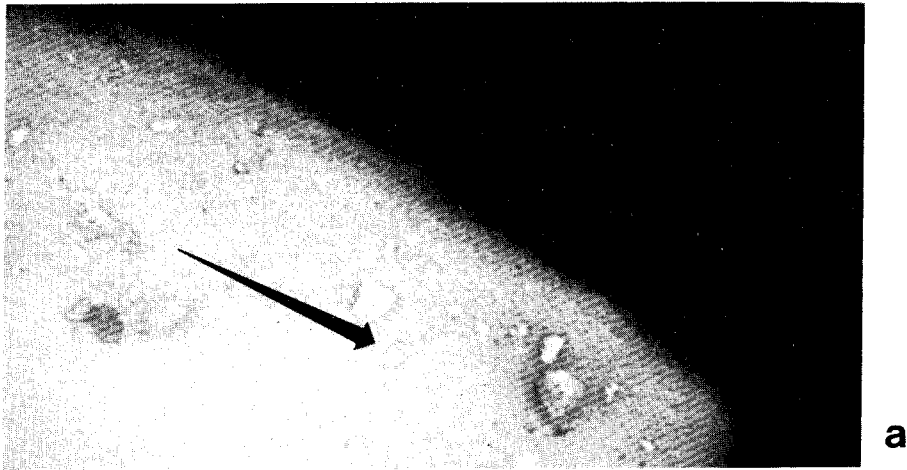


Plate VII. Test 4:

- a) The developed main channel contains initially a relatively homogeneous thin suspension of clay particles and aggregates of  $10\ \mu\text{m}$  together with scattered silt sized particles of quarts and mica
- b) Increased flow,  $10^{-4}\ \text{m/s}$ , opens the channel and the central part gets relatively free from particles
- c) At flow rates of  $10^{-3}\ \text{m/s}$  erosion is limited and particle transport concentrated to a few pathways' in the channel

# List of SKB reports

## Annual Reports

1977-78

TR 121

### **KBS Technical Reports 1 - 120.**

Summaries. Stockholm, May 1979.

1979

TR 79-28

### **The KBS Annual Report 1979.**

KBS Technical Reports 79-01 - 79-27.  
Summaries. Stockholm, March 1980.

1980

TR 80-26

### **The KBS Annual Report 1980.**

KBS Technical Reports 80-01 - 80-25.  
Summaries. Stockholm, March 1981.

1981

TR 81-17

### **The KBS Annual Report 1981.**

KBS Technical Reports 81-01 - 81-16.  
Summaries. Stockholm, April 1982.

1982

TR 82-28

### **The KBS Annual Report 1982.**

KBS Technical Reports 82-01 - 82-27.  
Summaries. Stockholm, July 1983.

1983

TR 83-77

### **The KBS Annual Report 1983.**

KBS Technical Reports 83-01 - 83-76  
Summaries. Stockholm, June 1984.

1984

TR 85-01

### **Annual Research and Development Report 1984**

Including Summaries of Technical Reports Issued during 1984. (Technical Reports 84-01-84-19)  
Stockholm June 1985.

1985

TR 85-20

### **Annual Research and Development Report 1985**

Including Summaries of Technical Reports Issued during 1985. (Technical Reports 85-01-85-19)  
Stockholm May 1986.

1986

TR86-31

### **SKB Annual Report 1986**

Including Summaries of Technical Reports Issued during 1986  
Stockholm, May 1987

## Technical Reports

1987

TR 87-01

### **Radar measurements performed at the Klipperås study site**

Såge Carlsten, Olle Olsson, Stefan Sehlstedt,  
Leif Stenberg  
Swedish Geological Co, Uppsala/Luleå  
February 1987

TR 87-02

### **Fuel rod D07/B15 from Ringhals 2 PWR: Source material for corrosion/leach tests in groundwater**

### **Fuel rod/pellet characterization program part one**

Roy Forsyth  
Studsvik Energiteknik AB, Nyköping  
March 1987

TR 87-03

### **Calculations on HYDROCOIN level 1 using the GWHRT flow model**

### **Case 1 Transient flow of water from a borehole penetrating a confined aquifer**

### **Case 3 Saturated-unsaturated flow through a layered sequence of sedimentary rocks**

### **Case 4 Transient thermal convection in a saturated medium**

Roger Thunvik, Royal Institute of Technology,  
Stockholm  
March 1987

TR 87-04

### **Calculations on HYDROCOIN level 2, case 1 using the GWHRT flow model**

### **Thermal convection and conduction around a field heat transfer**

### **experiment**

Roger Thunvik  
Royal Institute of Technology, Stockholm  
March 1987

TR 87-05

### **Applications of stochastic models to solute transport in fractured rocks**

Lynn W Gelhar  
Massachusetts Institute of Technology  
January 1987



TR 87-06

**Some properties of a channeling model of fracture flow**

Y W Tsang, C F Tsang, I Neretnieks  
Royal Institute of Technology, Stockholm  
December 1986

TR 87-07

**Deep groundwater chemistry**

Peter Wikberg, Karin Axelsen, Folke Fredlund  
Royal Institute of Technology, Stockholm  
June 1987

TR 87-08

**An approach for evaluating the general and localized corrosion of carbon steel containers for nuclear waste disposal**

GP March, KJ Taylor, SM Sharland, PW Tasker  
Harwell Laboratory, Oxfordshire  
June 1987